

Interaction between two contrasting magmas in the Albtal pluton (Schwarzwald, SW Germany): textural and mineral-chemical evidence

Lorenz Michel¹ · Thomas Wenzel¹ · Gregor Markl¹

Received: 8 April 2016 / Accepted: 21 June 2016 / Published online: 11 July 2016
© Springer-Verlag Berlin Heidelberg 2016

Abstract The magmatic evolution of the Variscan Albtal pluton, Schwarzwald, SW Germany, is explored using detailed textural observations and the chemical composition of plagioclase and biotite in both granite and its mafic magmatic enclaves (MMEs). MMEs probably formed in a two-step process. First, mafic magma intruded a granitic magma chamber and created a boundary layer, which received thermal and compositional input from the mafic magma. This is indicated by corroded “granitic” quartz crystals and by large “granitic” plagioclase xenocrysts, which contain zones of higher anorthite and partly crystallized from a melt of higher Sr content. Texturally, different plagioclase types (e.g. zoned and inclusion-rich types) correspond to different degrees of overprint most likely caused by a thermal and compositional gradient in the boundary layer. The intrusion of a second mafic magma batch into the boundary layer is recorded by a thin An₅₀ zone along plagioclase rims that crystallized from a melt enriched in Sr. Most probably, the second mafic intrusion caused disruption of the boundary layer, dispersal of the hybrid magma in the granite magma and formation of the enclaves. Rapid thermal quenching of the MMEs in the granite magma is manifested by An₃₀ overgrowths on large plagioclase grains that contain needle apatites. Our results demonstrate the importance of microtextural investigations for the reconstruction of possible mixing end members in the formation of granites.

Keywords Mafic enclave · Granite · Magma chamber processes · Magma mixing · Plagioclase · Schwarzwald

Introduction

While granitoid rocks form a significant portion of the continental crust, their petrogenesis and the origin of the observed chemical variability of these rocks are still under discussion. Both source region composition and processes (e.g. Chappell 1996; Clemens et al. 2009; Clemens and Stevens 2012) and the interaction between contrasting magmas and between magma and country rocks at the intrusion level (e.g. Barbarin 2005; Bateman et al. 1992; Neves and Vauchez 1995) add to their chemical variability.

Thermal, chemical and mechanical exchange can occur when two contrasting magmas interact (e.g. Barbarin and Didier 1992). The term “mixing” is used in the sense of combining, while mingling means “to move along while retaining an identity” (e.g. Pitcher 1997). Intense magma mixing results in hybridization of magmas (Barbarin and Didier 1992), which produces melts of intermediate composition (e.g. Eichelberger 1978; Reubi and Blundy 2009) such as calc-alkaline plutons showing I-type characteristics (e.g. Barbarin 2005; Sisson et al. 1996). Style and extent of interaction depend on the properties of the contrasting magmas (e.g. temperature, viscosity, composition, crystal content) and also their respective mass fractions (Sparks and Marshall 1986). Mafic magmatic enclaves (MMEs) in granites are thought to be the result of magma mingling (Didier and Barbarin 1991). Although magma mingling implies only physical dispersion of one magma in the other (Barbarin and Didier 1992), purely physical dispersion without any chemical exchange is not very common (Perugini and Poli 2012). Therefore, we use the term

Electronic supplementary material The online version of this article (doi:10.1007/s00531-016-1363-7) contains supplementary material, which is available to authorized users.

✉ Lorenz Michel
lorenz.michel@uni-tuebingen.de

¹ Department of Geosciences, University of Tübingen, Wilhelmstrasse 56, 72074 Tübingen, Germany

magma mixing in this work, meaning mechanical, thermal and chemical exchange between contrasting magmas.

Several textural characteristics may form “magma-mixing-compatible textural assemblages” as summarized by Hibbard (1991). Particularly, plagioclase has been used to unravel magma chamber processes such as magma mixing, heating or decompression in plutonic rocks (e.g. Blundy and Shimizu 1991; Pietranik and Koepke 2009; Pietranik et al. 2006; Pietranik and Waight 2008). The advantage of using mineral scale investigation methods is their fine spatial resolution, which can resolve single events and constrain possible mixing end members (Davidson et al. 2005).

Bulk rock and petrographical characteristics of endogenic enclaves in the Albtal pluton, Schwarzwald, southern Germany, have been provided by Wimmenauer (1963) and Stenger (1979). We now use microtextural and mineral-chemical data of plagioclase, biotite, quartz and apatite to reconstruct magma chamber dynamics (see, e.g. Singer et al. 1995). The major aim is to study effects of the interaction of two contrasting magmas on the observed

compositional variability of a granite and its enclaves in detail.

Geology of the study area

The Schwarzwald in SW Germany is part of the European Variscan Belt and mostly composed of metamorphic/migmatitic and magmatic rocks. It consists of three major tectonic units (Eisbacher et al. 1989). Rocks of the Saxothuringian Belt can be found in the northern Schwarzwald, whereas the Central Schwarzwald Gneiss Complex (CSGC) and Southern Schwarzwald Gneiss Complex (SSGC) dominate the central and southern Schwarzwald (see Fig. 1). Lower Carboniferous collision between CSGC and SSGC was followed by slab breakoff, nappe-stacking and high-temperature (HT) metamorphism (Hann et al. 2003; Hegner et al. 2001). Eclogite-grade metamorphism was dated to 345–335 (Kalt et al. 1994), and HT-metamorphism and widespread anatexis occurred around 335–330 Ma

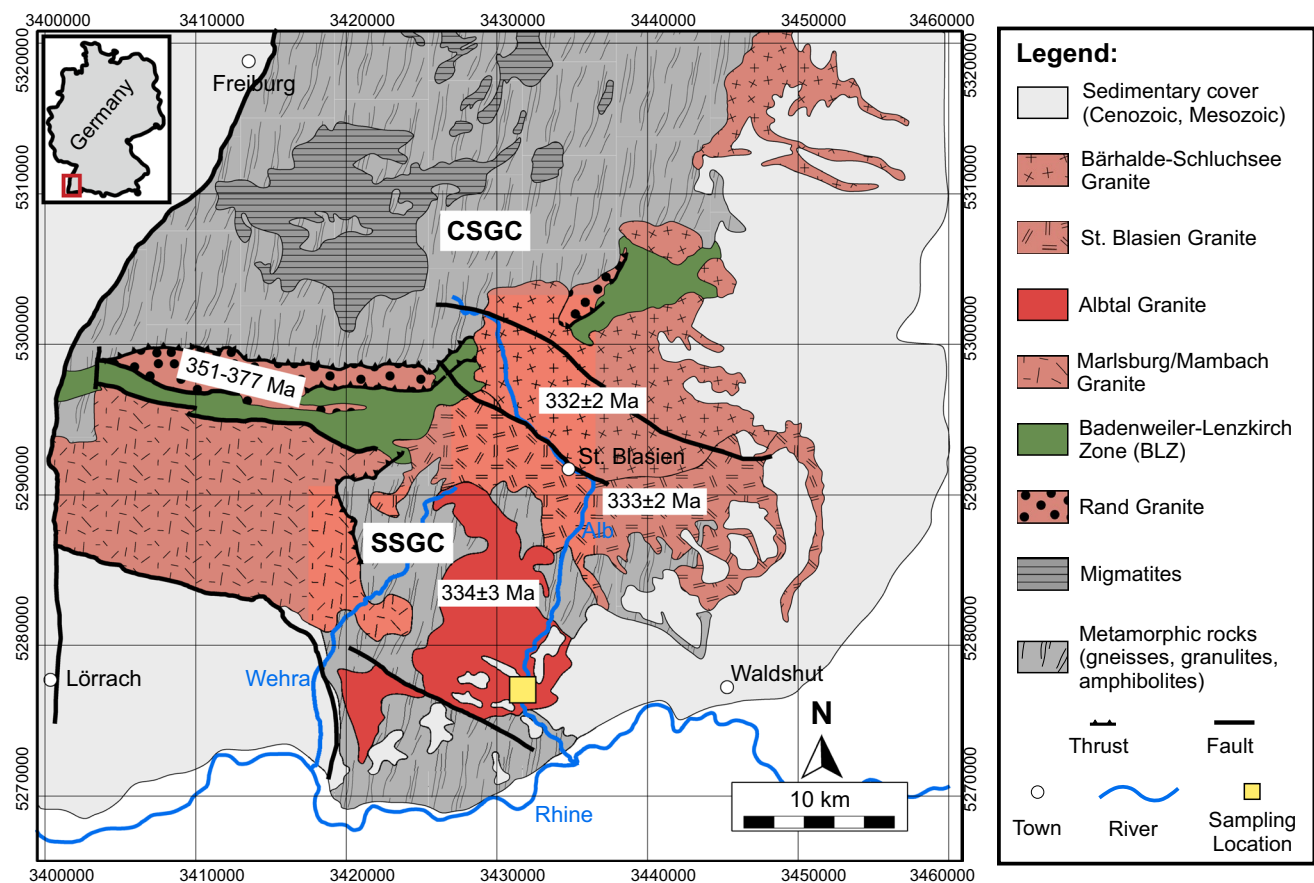


Fig. 1 Regional geology of the southern Schwarzwald; ages for the granites are from Hann et al. (2003) and Schaltegger (2000), CSGC Central Schwarzwald Gneiss Complex, SSGC Southern Schwarzwald Gneiss Complex. The sampling location of the analysed granite and

enclave samples from the active quarry Tiefenstein is indicated. Coordinates (in degree and decimal minutes, WGS 84) are N47 37.808, E08 05.652, and coordinates on the map's grid are Gauss–Krüger coordinates. *Map* is based on geological map of Baden-Württemberg

Table 1 Short description of the investigated samples

Sample name	Rock type	Description and peculiarities	Analyses
LM 22	Granite	Normal, coarse-grained granite	TS, MP, XRF
LM 23	Granite	With large alkali feldspar, containing concentric biotite-rich regions	TS, MP
LM 27	Granite	Fine-grained granite with rapakivi feldspar	TS, MP, XRF
LM 32	Granite	Usual granite	XRF
LM 33	Granite	Fine-grained granite, but also with coarser areas, no rapakivi feldspars	XRF
LM 24	Enclave	With large quartz crystals and biotite agglomerations, sharp contact towards granite	XRF
LM 25	Enclave	Contains abundant large biotite crystals, gradual transition towards granite	TS, MP, XRF
LM 28	Enclave	Contains a gneissic inclusion, sharp contact to granite	TS, MP
LM 36	Enclave	Very fine-grained, contains one large alkali feldspar and abundant large crystals of rounded quartz (with dark seam)	XRF
LM 41	Enclave	Large enclave (30 cm diameter), with rim-to-core profile (three individual samples), abundant crystals of quartz, biotite and plagioclase, contains mafic xenolith inclusion, sharp contact towards granite	TS, MP, XRF
LM 42	Enclave	Large enclave (50 cm diameter), with large alkali feldspars and biotites, sharp contact towards granite	TS, MP, XRF

TS thin section, *MP* microprobe, *XRF* X-ray fluorescence analysis

(Marschall et al. 2003). During the post-collisional exhumation and uplift, numerous S-type granitic plutons intruded at mid-crustal levels (Eisbacher et al. 1989; Schaltegger 2000) for which a metapelitic crustal source is assumed (Hoefs and Emmermann 1983; Liew and Hofmann 1988). Melting was likely caused either by underplating of mantle-derived melts or by asthenosphere upwelling associated with delamination (Büttner and Kruhl 1997; Marschall et al. 2003). The granites in the southern Schwarzwald have very similar ages (332–334 Ma) and almost overlap with the HT-metamorphism (Schaltegger 2000).

The Albtal granite is situated at the southern border of the Schwarzwald (Fig. 1). In contrast to other granite plutons of the southern Schwarzwald (e.g. the Bärhalde-Schluchsee, St. Blasien, Malsburg granites), it is the only granite with mafic enclaves of tonalitic to granodioritic composition (Stenger 1979) and it shows tendencies towards an I-type character (molar $\text{Al}_2\text{O}_3/(\text{CaO} + \text{Na}_2\text{O} + \text{K}_2\text{O}) < 1.1$; Emmermann et al. (1975). The Albtal granite is chemically zoned ranging from a more primitive composition in the SE to a more evolved composition in the NW, which Emmermann (1968) attributed to magmatic differentiation.

Analytical methods and selected samples

Major and trace elements were analysed with a Bruker AXS S4 Pioneer XRF device as described by Eroglu et al. (2015). The results can be found in the electronic supplement A1.

In situ chemical analysis of feldspar and biotite were performed using a JEOL 8900 Superprobe at the University of Tübingen. The accelerating voltage was 15 kV and the beam current 20 nA. For major elements, the counting

time was 16 s on the peak and 8 s on each background. Profiles in feldspar were investigated for their trace element variations (Sr, Ba, Fe), using a current of 40 nA and longer counting times. Natural and synthetic standards were used for the calibration. Detection limits and standard deviations as well as a representative set of mineral analyses can be found in the electronic supplement A2.

Due to dense vegetation, fresh bedrock outcrops are very rare. Fortunately, the active quarry near Tiefenstein provides an excellent opportunity for sampling freshly blasted material. Table 1 gives an overview of the samples, macroscopic peculiarities and the performed investigations.

Granite samples comprise two types. Coarse-grained granites contain large alkali feldspar crystals (up to several cm, Fig. 2a) in a coarse-grained (about 1 cm) matrix of quartz, plagioclase, biotite and minor alkali feldspar. Fine-grained granites have a fine matrix containing biotite and well-rounded crystals of plagioclase, quartz and alkali feldspar several mm in size. Large rapakivi-type feldspars are observed in the fine-grained granite type only. They can occur next to non-rapakivi grains in the same sample.

Mafic enclaves are well rounded to oval shaped, and their size can vary considerably ranging from 5 to 50 cm in diameter (Fig. 2b). Enclaves can contain other enclaves (Fig. 2c), but also mafic and gneissic xenoliths. With the exception of sample LM 25 (Fig. 2d), the contact of all mafic enclaves towards the granite is sharp (Fig. 2e) and no chilled margin or rim with accumulation of a preferred mineral (e.g. like biotite rinds, Farner et al. 2014) is developed. The mafic enclaves have a fine-grained matrix (Fig. 2e) containing biotite, plagioclase and quartz. There are distinctly larger crystals (up to 5 cm in size) of alkali feldspar, biotite, plagioclase and quartz embedded in this matrix.

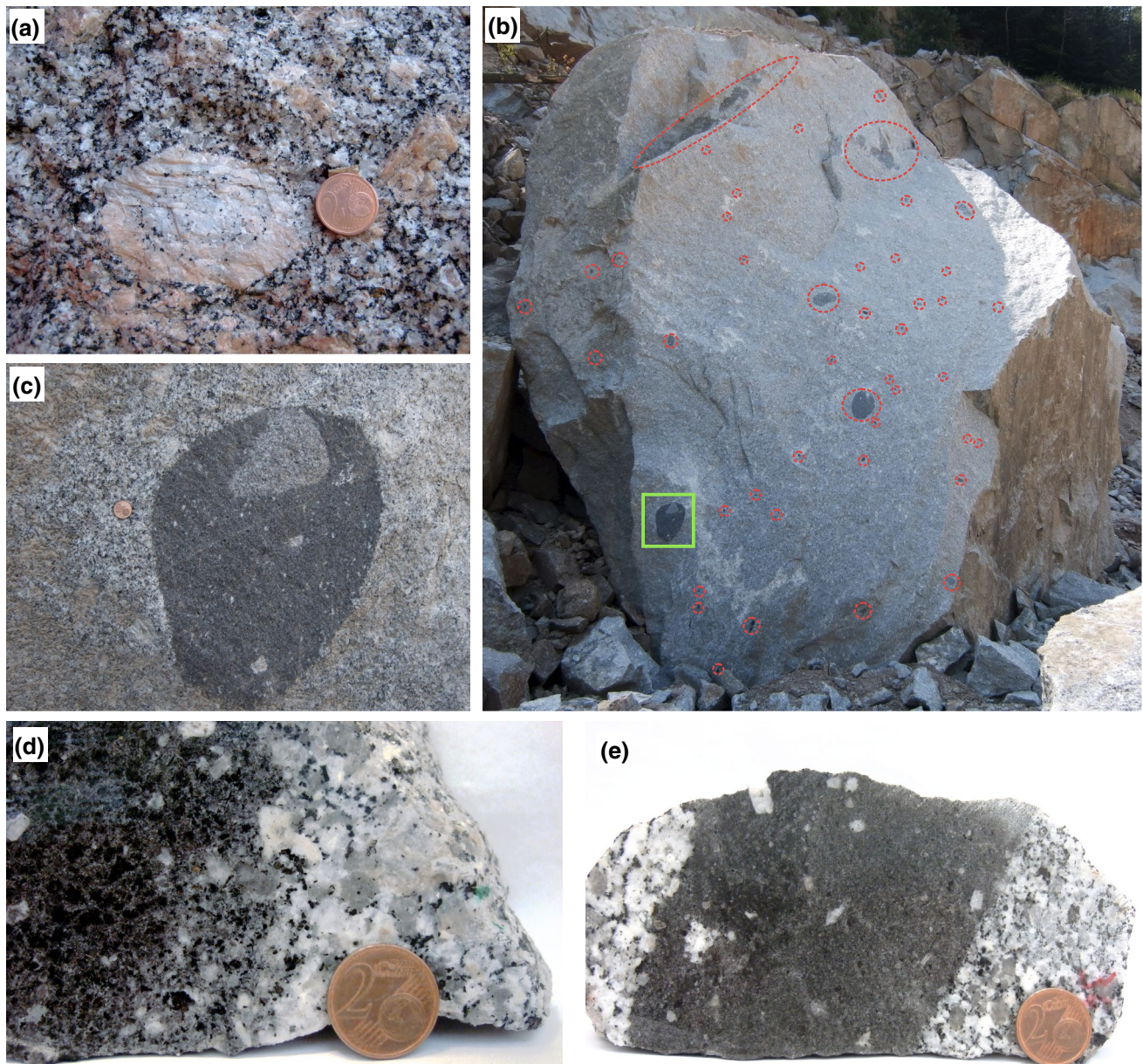


Fig. 2 **a** Albtal granite with large, euhedral alkali feldspar. **b** Freshly blasted granite boulder with abundant enclaves of varying size (*red circles*), most enclaves have a rounded shape, enclave in the *green box* is further depicted in *2c*, and height of the boulder is 4 m. **c** Close-up view of an enclave with rounded shape, fine-grained matrix

and coarser grains of plagioclase, alkali feldspar and biotite; the enclave is intermingled with granite. **d** Enclave sample LM 25, with more gradual contact towards the granite. **e** “Normal” enclave with sharp contact towards the granite. *Coin* in all images is 18 mm in diameter

Chemical composition of enclaves and granite

Figure 3 displays the range of chemical composition of mafic enclaves and granites, using our own data and analyses of Stenger (1979) and Emmermann et al. (1975). In general, the SiO_2 content of the mafic enclaves ranges between 58 and 68 wt% and can be as high as in the

granite. Al_2O_3 increases with decreasing SiO_2 content; however, a well-defined trend is not developed and two biotite-rich samples have significantly lower Al_2O_3 contents. TiO_2 , MgO and Fe_2O_3 decrease with increasing SiO_2 , defining a rough trend between two possible end members. Deviations are again caused by biotite-rich samples. All enclaves have lower K_2O contents than the

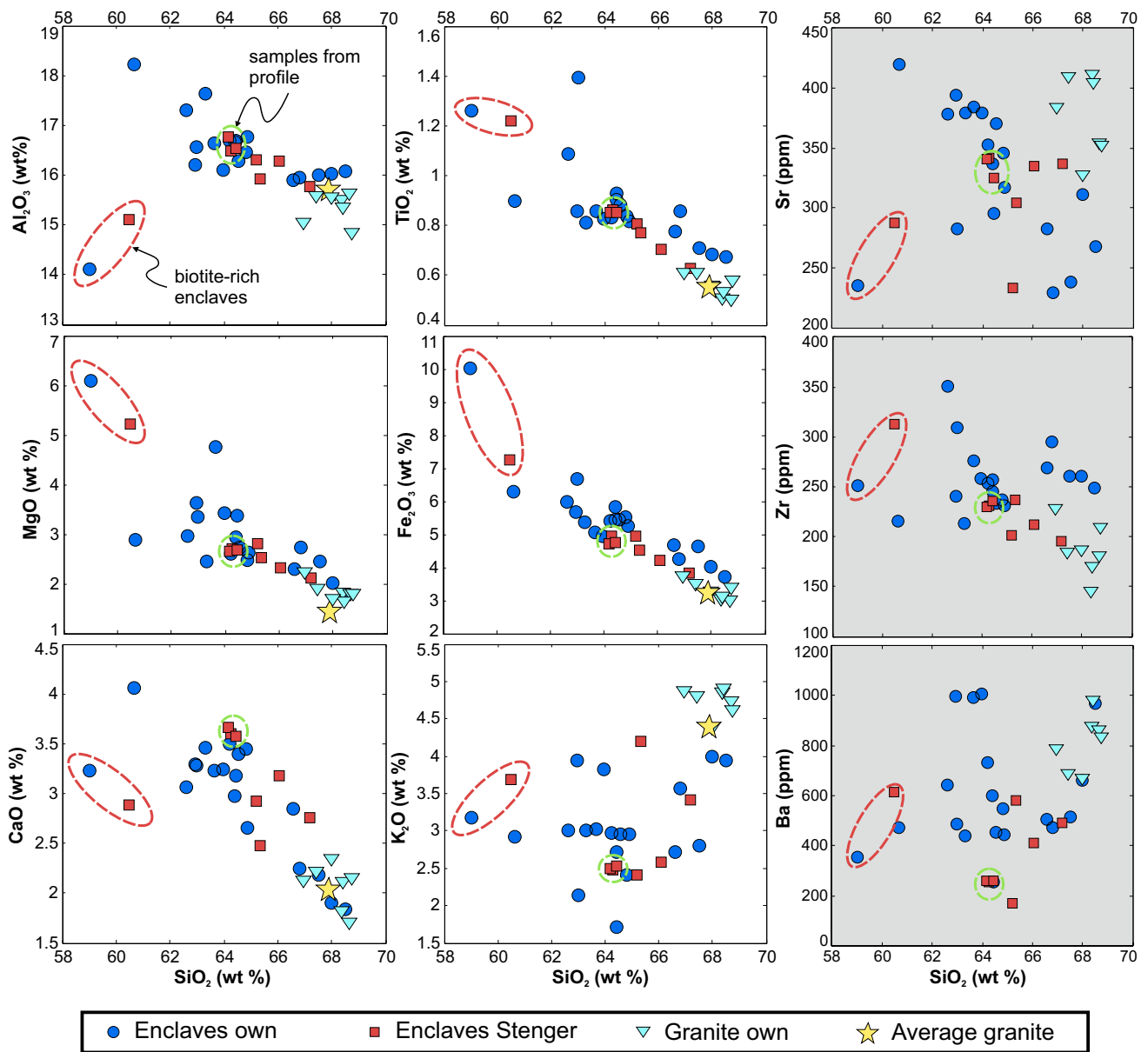


Fig. 3 Harker-plots of major (Al, Ti, Mg, Fe, Ca, K) and trace elements (Sr, Ba, Zr, grey panels) of the Albtal granite and its enclaves. Average granite composition is from Emmermann et al. (1975), other

enclave data from Stenger (1979). Biotite-rich enclaves (red ellipse) and samples from the rim-to-core profile (green ellipse) are indicated

granite samples and no clear correlation with the SiO₂ content exists. The compositional variation between different mafic enclaves is much larger than the variation inside a single enclave as revealed by a rim-to-core profile (about 20 cm in length) performed in sample LM 41, where the three sample splits completely overlap in composition (green ellipse in Fig. 3). Trace element data do not follow trends but show a large scatter when plotted against silica (Fig. 3). Although lower in SiO₂, many enclaves are as rich in Sr as the granite. Zr is higher in

almost all enclave samples compared to the granite. Ba tends to be lower in the enclaves, but some enclaves are as rich in Ba as the granite samples.

Possible mixing end members of MMEs are typically constrained from the chemical (and isotopic) variation in bulk composition of MMEs (e.g. Waight et al. 2001), assuming that the enclaves represent mixtures of two melts. However, the crystal cargo during mixing plays a significant role and is responsible for deviations from “perfect mixing trends” (see, e.g. Ubide et al. 2014).

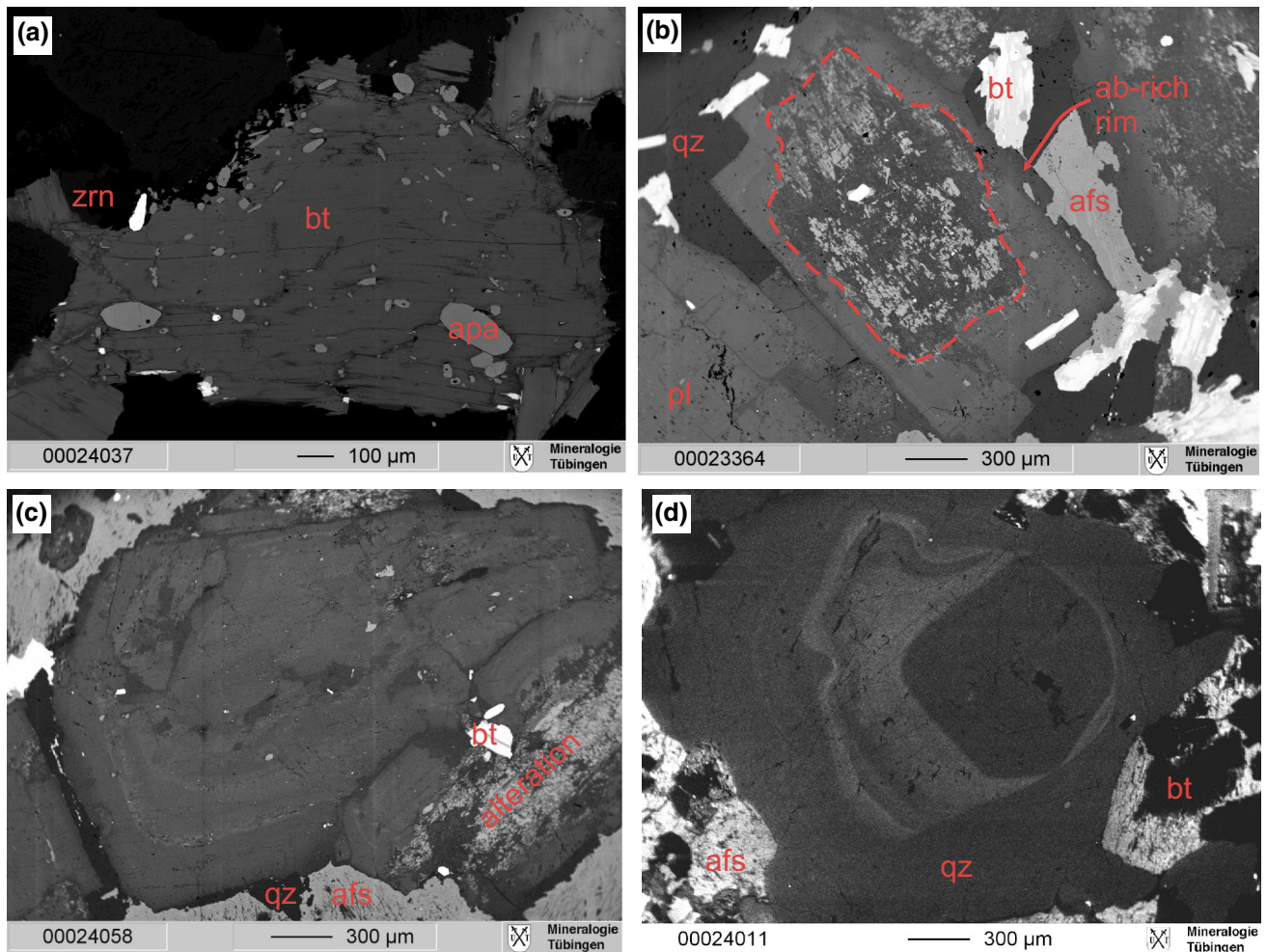


Fig. 4 BSE and CL images of typical textures observed in the granite, **a** biotite (bt) with inclusions of apatite (apa), and zircon (zrn), **b** plagioclase (pl) with strongly altered core and thin, albite-rich (ab)

rim, aside with quartz (qz) and alkali feldspar (afs), **c** zoned plagioclase with unaltered core and minor inclusions, **d** quartz in the coarse-grained granite with complex growth pattern

Microtextural characteristics of biotite, plagioclase and quartz

Granite

In both granite types, biotite is either present as large euhedral grains (1–5 mm), containing abundant inclusions of apatite, monazite and zircon (Fig. 4a), or as smaller, subhedral-to-anhedral grains filling the space between the other phases.

Plagioclase is a major phase in the granite and occurs as large (several mm up to one cm) euhedral grains. Although some plagioclase crystals are altered to zoisite and albite, two main plagioclase types can be observed: a slightly zoned type with altered cores (Fig. 4b) or with unaltered core (Fig. 4c) and glomerocrystic grains (cf. Hogan 1993). The latter consists of several individual plagioclase grains

attached to each other by irregular, embayed contacts. The individual grains show concentric zonation. Both types occur in the coarse- and fine-grained granite types.

In the coarse-grained granite, quartz is either present as large, subhedral grains (3–10 mm) or as small, anhedral grains, filling the space between other phases. Some grains have complex cathodoluminescence (CL) patterns with rounded and embayed growth zones. Number of growth zones and intensity of overprint are variable (Fig. 4d). Other grains display a more regular CL pattern. Large well-rounded grains (several mm in size) as well as small angular crystals are present in the matrix of the fine-grained granite. Large quartz grains show either irregular CL patterns with zones of variable thickness or homogeneous patterns with well-defined growth zones. Their edges are sometimes rounded, and they have thin (5–10 μm) and bright rims. Matrix quartz crystals do not show any zonation.

In the coarse-grained granite, large euhedral alkali feldspar crystals often contain concentrically arranged inclusions of biotite, quartz and plagioclase. Rapakivi-type feldspar in the fine-grained granite consists of an alkali feldspar core mantled by a plagioclase rim broader than 1 mm. The rim consists of individual, zoned plagioclase grains and minor amounts of quartz. Anhedral alkali feldspar grains, poikilitically enclosing other phases, are ubiquitous in the matrix of the fine-grained granite.

Enclaves

Matrix

The enclaves' matrix is fine-grained (100–500 μm) and consists dominantly of tightly intergrown plagioclase, biotite and quartz. The mean volumetric mineral contents determined by BSE imaging are plagioclase 59 %, quartz 26 %, biotite 14 %, alkali feldspar <1 % and apatite <1 % which would correspond to an IUGS tonalite (LeMaitre 2002). Biotite shows a lathlike, elongated shape, ranging from anhedral to euhedral plates. Plagioclase tends to more equilateral grains approximating a euhedral grain shape. It builds up a framework with all the other phases in the interstices. Most plagioclase crystals are zoned and contain altered cores. Anhedral quartz either fills up the interstices between plagioclase and biotite or poikilitically encloses all other phases, suggesting a late growth of quartz in the enclaves' matrix. Alkali feldspar is usually rare in the matrix and a late-stage phase, being either present in the interstices between the other matrix phases or enclosing them. High contents of matrix alkali feldspar were only observed in enclaves with either a gneissic xenolith or large alkali feldspar xenocrysts. Particular needle apatites with extreme aspect ratios of up to 80:1 are commonly enclosed by all other matrix minerals.

Coarse-grained minerals

Large biotite grains can be divided into three different types based on their textural characteristics (see Fig. 5 and Table 2 for more details). Large inclusion-rich biotite is the most common type (Fig. 5a), whereas biotite clusters are less frequent (Fig. 5b, c). The reaction-type biotite was only observed in a reaction rim around a mafic xenolith or together with quartz, amphibole and sulphide minerals in a reaction texture (Fig. 5d).

Large plagioclase crystals (1–5 mm) can be divided into zoned, inclusion-rich and core types (see Fig. 6 and Table 3). The zoned plagioclase type is inclusion-poor and characterized by different zonation patterns. Oscillatory and more complex patterns occur (Fig. 6a). The most abundant plagioclase is the inclusion-rich type, characterized by

numerous inclusions in a patchily zoned plagioclase. It is variable in appearance but in the most commonly observed pattern, three different domains can be distinguished. The central parts of the grains contain irregularly shaped cores, followed by the inclusion-rich zone exhibiting patchy zonation and a broader low-An rim containing needle apatites (Fig. 6b). The most common inclusions are biotite, alkali feldspar, albite-rich plagioclase and quartz, but Fe-rich sulphides, apatite, allanite, titanite and scheelite were also observed. Core-type plagioclase grains have strongly altered cores (Fig. 6c). These crystals are inclusion-poor and show a weak zonation in some cases.

Large quartz grains between 1 and 3 mm size have a distinctly inclusion-free interior, followed by a rim with many tiny (50–300 μm) biotite inclusions and needle apatites (Fig. 7a). Rounded quartz cores often show internal CL zonation (Fig. 7b). Resorption embayments can be present, ranging from the rim into the zoned cores. At the base of the biotite- and apatite-rich rim, there is a thin, dark seam, sometimes preceded by a thin bright seam (Fig. 7b) with many small embayments.

Based on the typical magmatic characteristics, the lack of cumulus textures and the high content of biotite, the Albtal enclaves will in the following be termed mafic microgranular/magmatic enclaves (MMEs, Didier and Barbarin 1991). The observed complexity of the plagioclase grains is also at odds with the smooth, regular normal zonation of plagioclase typical for cumulate material (Brophy et al. 1996). Instead, these textures suggest a very dynamic environment during their genesis.

Mineral chemistry of biotite and plagioclase

Biotite

The texturally different biotite types of the MMEs (Table 2) can also be distinguished chemically (Fig. 8 and electronic suppl. A2). Most of the reaction-type biotites show more primitive compositions (#Fe 0.36–0.44) than the other types. Matrix, cluster and large biotites of the MMEs are very similar in terms of their #Fe and Ti content. Large biotite grains in MMEs show distinctive characteristics of granitic biotite in terms of higher Ba, overlapping Ti contents and similar #Fe.

Plagioclase

Results of single-spot analyses of the different plagioclase types are summarized in Fig. 9, and representative data can be found in electronic supplement A2. Plagioclase grains in the coarse-grained granite mostly show a rather narrow composition between An₂₇ and An₃₁ with a median of An₃₀.

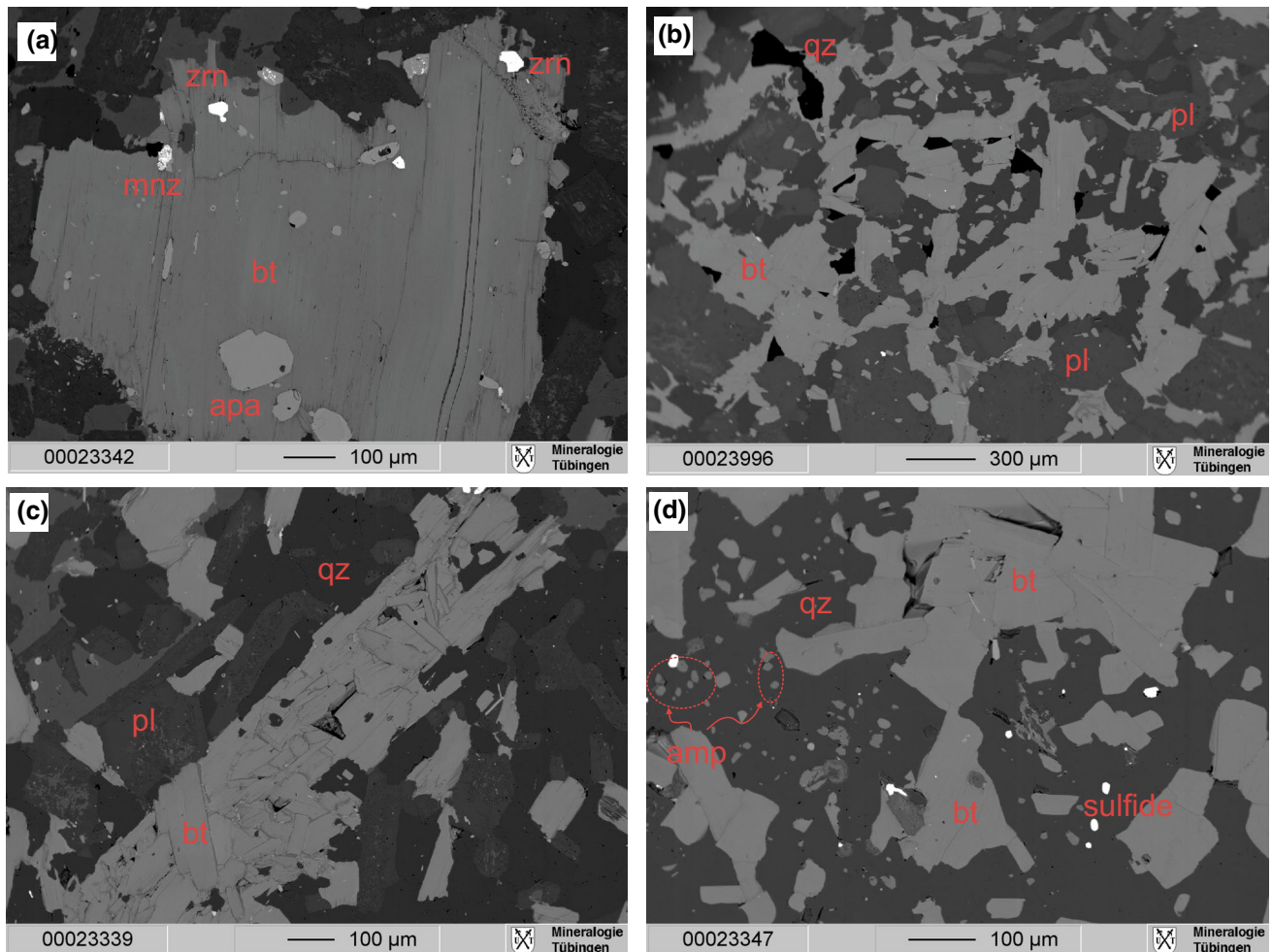


Fig. 5 BSE images of biotite types in MMEs, **a** large type containing many inclusions of apatite, monazite (mnz) and zircon, **b** loosely packed cluster type with interstitial plagioclase and quartz, **c** tightly

packed cluster type, almost devoid of interstitial minerals, **d** reaction-type biotite intergrown with quartz that contains small inclusions of amphibole (amp) and sulphide grains

Lower An contents as low as An₅ may be caused by hydrothermal alteration. Compared to the coarse-grained granite, plagioclase in the fine-grained granite shows a tendency towards higher An contents, especially matrix grains.

Matrix plagioclase grains of the MMEs have a rather restricted composition of An₃₀–An₃₅ with a median of An₃₂, being similar to the average granite composition. From inclusion-rich type to zoned- and core-type plagioclase, the average An content successively rises (median of An₃₄, An₃₈ and An₄₇, respectively), but also the compositional variability increases.

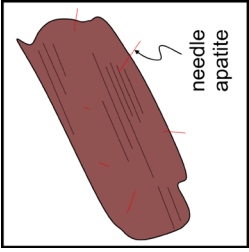
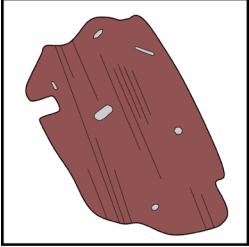
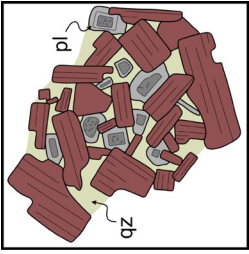
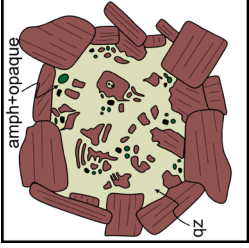
Chemical profiles in large plagioclase grains of granite and MMEs are displayed in Fig. 10 and show the measured An and Sr content and the calculated Sr content of the melt (Sr_{melt}) the plagioclase grain was assumed to be in equilibrium with. Sr_{melt} was calculated using the distribution coefficient of Blundy and Wood (1991), assuming a temperature of 900 °C based on results of melting experiments on

a granodioritic enclave from the Albtal pluton (Büsch and Otto 1980). A more thorough elaboration of parameters influencing the An content and Sr_{melt} of plagioclase can be found in the discussion section.

A compositional profile through a zoned plagioclase from the coarse-grained granite (Fig. 10a) shows a core of An₃₀, followed by a more abrupt increase up to An₃₈ in a distinct zone close to the rim, and a return to the An₃₀ value within 20 μm of the profile. In general, the Sr content of the crystal decreases from core (1000 ppm) to rim (500 ppm). The Sr variation does not mirror the zonation visible in the An profile, but some regions with high An contents also show high Sr contents. The calculated Sr_{melt} content in the melt decreases from 140 ppm in the core down to 50 ppm in the rim but the rise in An content at the rim is not associated with a rise of the calculated melt's Sr content.

In a zoned-type plagioclase crystal from the MME (Fig. 10b), irregular patches with An contents between An₃₈

Table 2 Overview of the different biotite types within the enclaves

Type	Matrix	Large	Type	Cluster	Reaction
Description	Small grains (100–400 μm), shape varying from anhedral to euhedral (often lathlike, elongated grains), with needle apatites	Single, large (1 mm) grains, euhedral to subhedral, platy/tabular shape, inclusions of zircon and apatite		Clumps of biotite, either tightly packed (anhedral grains) or more loosely packed (subhedral, tabular/lathlike grains, with interstitial quartz and plagioclase), sometimes larger apatite grains are included in the biotite	Vermicular intergrowth of biotite with quartz, small grains of amphibole and opaque phase inside the quartz, strong sign of disequilibrium Biotite associated with amphibole (and minor quartz) in the amphibole-rich, mafic inclusion
Appearance					
Occurrence in enclave	Important constituent of the groundmass	Frequent, dominant type		Medium	Rare, but very frequent in LM 25 sample
Occurrence in granite	Not observed	Frequent, dominant type		Not observed	Very rare

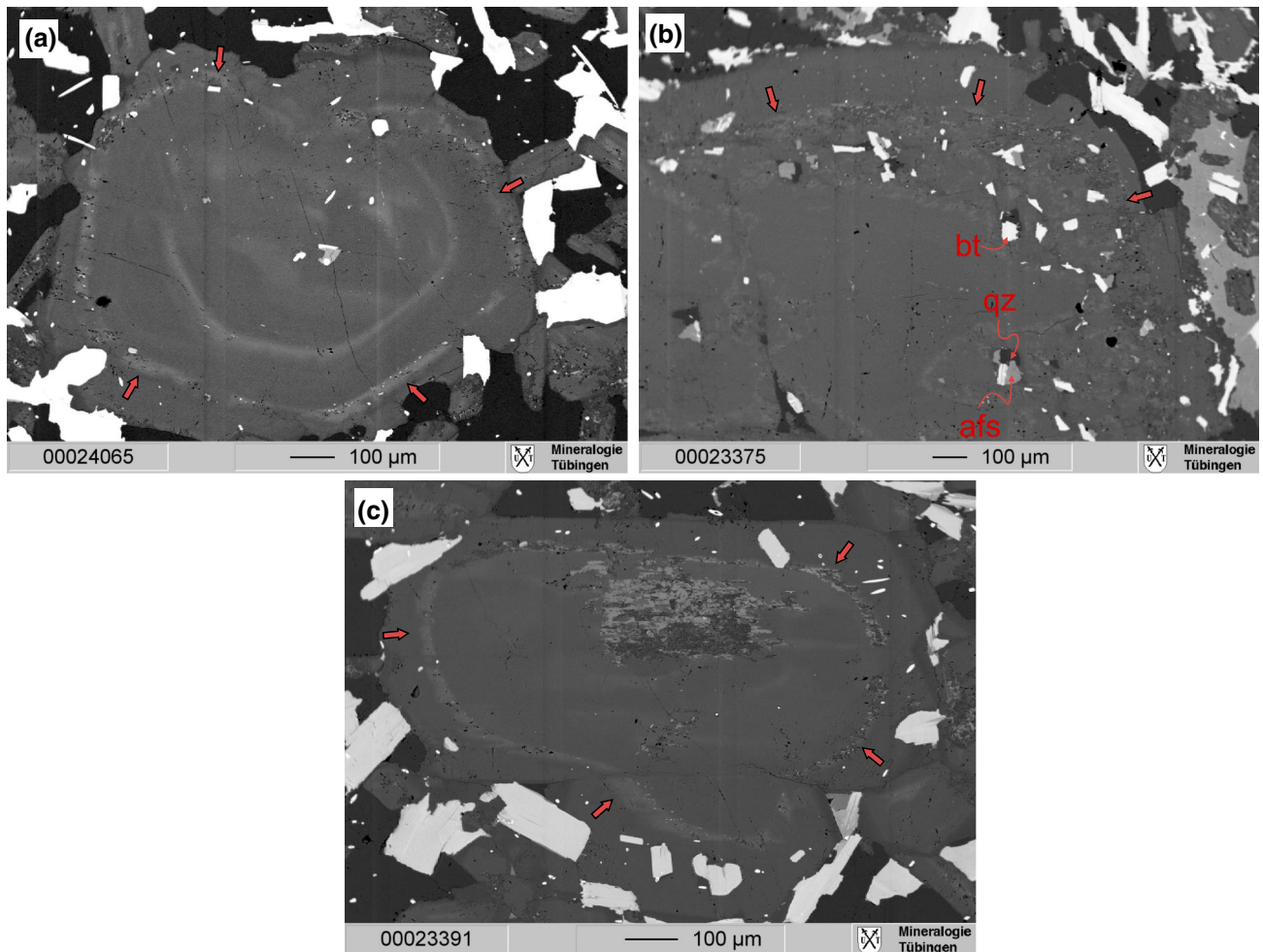


Fig. 6 BSE images of the different plagioclase types in MMEs, **a** zoned type with patchy interior and concentric zoning at the rim, **b** inclusion-rich type with inclusions of biotite, quartz and alkali feldspar, **c** core type with strongly altered An-rich core, surrounded by

low-An plagioclase. In all images, the different types have a thin, high-An seam close to the rim (partly interrupted, marked by *red arrows*)

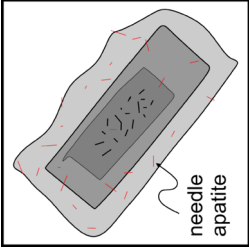
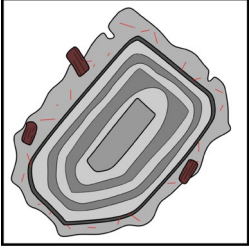
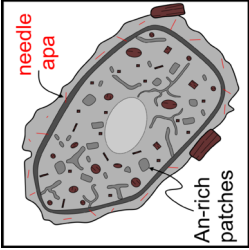
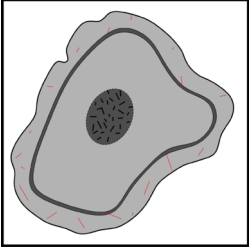
and An₄₅ occur in the core. A thin zone is attached with an abrupt increase up to An₄₈ and a more gradual decrease down to An₃₀; oscillations between An₃₀ and An₃₈ dominate the following part towards the rim of the crystal. The rim starts with an interrupted zone of An₄₉, followed by a decrease in the An content back to An₃₀. The Sr concentration in general decreases from 1000 ppm in the core down to 400 ppm in the rim. Zones of high An content often coincide with high Sr concentrations. The calculated Sr_{melt} content is highest at the thin An₄₉ seam in the rim and within the An₄₅ zone in the core of the crystal.

Where developed, the core of inclusion-rich plagioclase in MMEs varies between An₃₀ and An₄₀. In a grain with completely resorbed core, single patches of the patchily zoned area can reach An₆₀; outside the area with patchy zoning, the plagioclase shows a rather constant composition of An₃₀–An₃₃ (Fig. 10c). In the rim the An

content again rises up to a thin seam with An₅₀ and afterwards decreases to An₃₀ in the outermost part of the crystal. The Sr concentration decreases from 1100 ppm in the core to 500 ppm and increases in the surroundings of the An₆₀ patch to 800 ppm. In the inclusion-free zone, there is a general decrease from approximately 800–400 ppm Sr. Although no strong increase in the Sr concentration is exhibited within the thin An₅₀ seam of this profile, another profile in the same grain shows an increase up to 800 ppm Sr in the An₅₀ seam. Highest Sr_{melt} values are calculated for the An-rich patch (200 ppm) and the An₅₀ seam (150 ppm, for the second profile in the crystal).

Analyses inside the core of a core-type plagioclase vary between An₆₅ and An₇₀ (not shown). The zone between core and rim shows an irregular pattern with areas of high An content (An₃₈–An₄₅) and a mean An₃₀–An₃₅ composition (Fig. 10d). The rim begins with an An₄₅–An₅₀ seam

Table 3 Overview of the different plagioclase types within the enclaves

Type	Matrix	Zoned	Inclusion-rich	Core
Description	Small (100–500 μm), zoned (usually concentric, partly dendritic), low-An seam, needle apatite in the entire grain, often altered in the centre (An-rich area of grain)	Large crystals (up to 2 mm), well developed concentric zonation (sometimes oscillatory), extent of zonation varies between the crystals, no biotite inclusions (alkali feldspar is possible)	Countless tiny biotite inclusions (often rounded, subordinate alkali feldspar, quartz and albite), patchy zonation (subordinate concentration), variable appearance (with or without inclusion-free core)	Rounded, strongly altered core, surrounded by broad, alteration-free (and often zoned) seam
Rim	No rim developed	In all three types: thin, high-An seam, followed by outermost low-An seam, both zones contain needle apatites		
Appearance				
Occurrence in enclave	Dominant constituent of the groundmass	Common	Frequent, dominant plagioclase type	Rare
Occurrence in granite	Not observed	Very often	Not observed	Varieties with strongly altered core exist

of variable thickness, but the An content rapidly decreases towards a dominating composition of An₃₀. In the zone between core and rim, the Sr content varies from 400 to

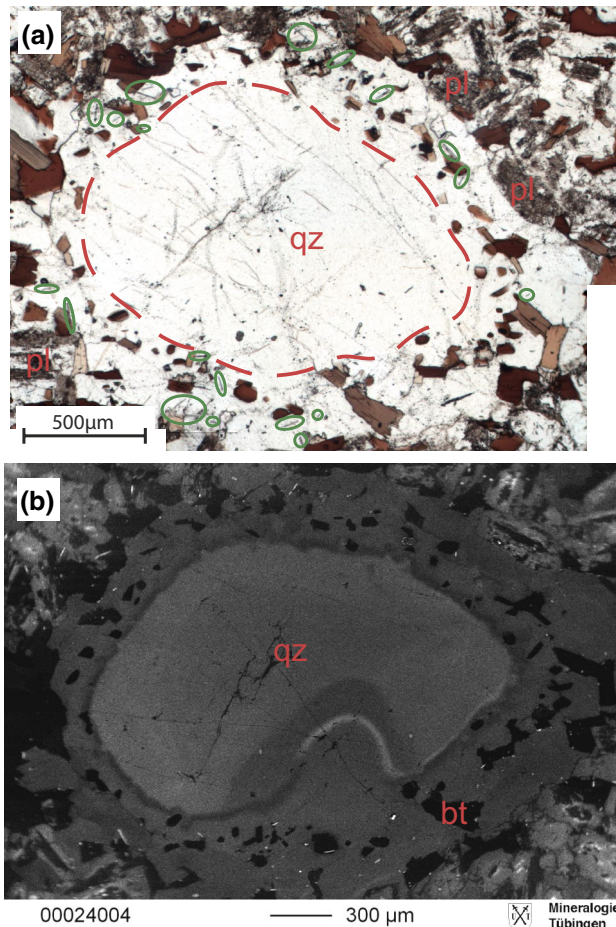
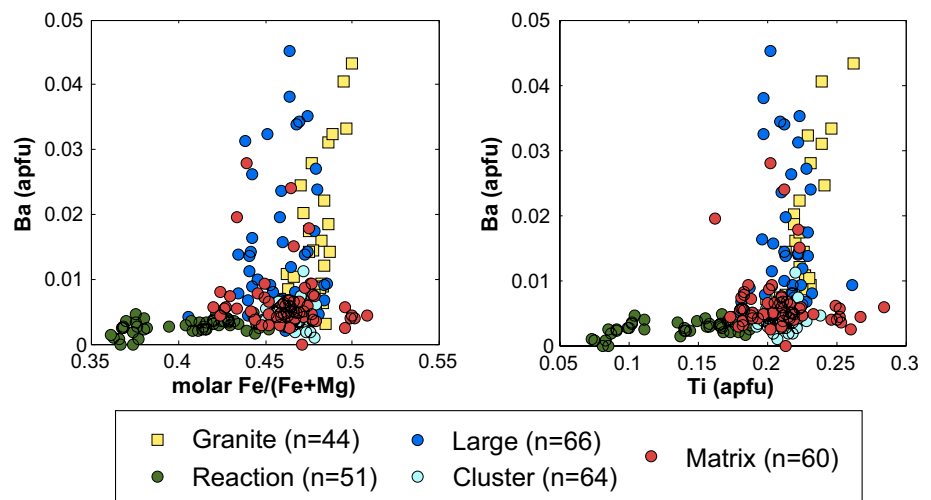


Fig. 7 Quartz textures in the enclaves, **a** photomicrograph (plane polarized light) of a grain showing an inclusion-free interior, overgrown by a rim containing inclusions of biotite and needle apatites (green circles), **b** CL image of the same grain as in **a**, a resorption embayment is developed in the lower part of the core

Fig. 8 Comparison of the different biotite types in MMEs (circles) and the granite (squares) in terms of their Ba versus #Fe and Ti content. Note that large biotite grains in the MMEs are similar to granitic biotite



800 ppm in the more An-rich zone. With the onset of the An₄₅–An₅₀ seam, a rise in the Sr concentration is observed, followed by a decrease to An₃₀ at the end of the profile. Calculated Sr_{melt} is high where the An content is high, and highest values are calculated for the An₄₅–An₅₀ seam.

A profile (not shown) through a matrix plagioclase lacks oscillatory zonation or strong signs of resorption. Instead, three compositionally distinct zones are developed. The core of the crystal is made up of An₄₅–An₅₀, the next outward seam has an An₃₀–An₃₅ composition and the outermost part consists of An₂₀. The lack of resorption features and the abrupt transition between the single zones is a remarkable difference to the larger, zoned plagioclase crystals in the MMEs, although their compositional range is similar. The Sr content of the crystal and calculated Sr_{melt} are rather constant in the An₃₀ and An₅₀ zones, and both decrease towards the rim.

In general, the dominating granitic plagioclase composition of An₃₀ is also found in different zones of the coarse-grained plagioclase types in MMEs. Despite of their complex interior, the rims are coherently composed of a thin An₅₀ seam with a higher calculated Sr_{melt} followed by a zone of An₃₀ and decreasing Sr_{melt} values.

Discussion

MMEs in the Albtal granite originated by magma mixing

One major argument that MMEs in the Albtal pluton are formed by interaction of two different magmas is the occurrence of elongated, blade-like biotite, needle apatite and quartz with concentrically arranged inclusions. These are typical textural features of igneous rocks associated with magma mixing (Hibbard 1995). Particularly, the formation of needle apatites records thermal quenching

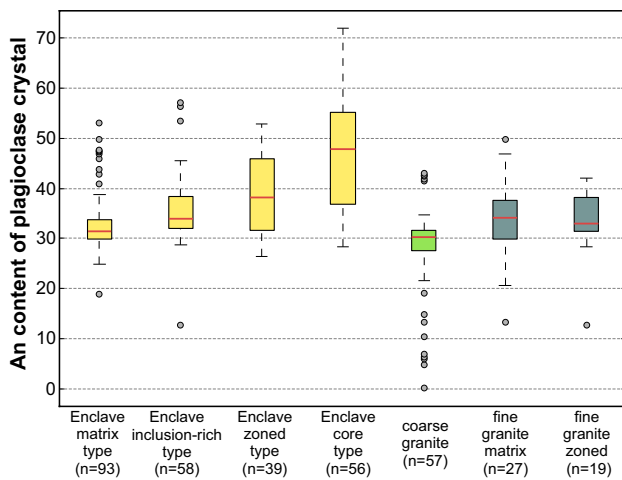


Fig. 9 Overview of the composition of the different plagioclase types in MMEs and the granite in terms of their anorthite (An) content. The red line in the boxes corresponds to the median An content, grey circles correspond to outliers (using 1.5 interquartile range for the end of the whiskers), and number n of analyses for each type is indicated

of the enclaves' parental magma (in contrast to, e.g. pressure quenching, Flood and Shaw 2014). The complexity of observed textures, i.e. reaction and resorption features in quartz and plagioclase as well as the coincidence of plagioclase regions of higher Sr_{melt} and higher An content, can also be explained by the thermal and chemical influence of a more mafic magma (see below). This mixing hypothesis is supported by isotope investigations in the Albtal granite and its mafic enclaves which documented Sr-isotopic disequilibrium between K-feldspar and plagioclase fractions (Schuler 1983). However, the samples used in the isotope study were mixtures of several minerals and not the spatially resolved methods used here.

The felsic magma can be identified as a “normal” unmodified (S-type?) granite since relics of “granitic” quartz and plagioclase (Figs. 6, 7) were found in the MMEs. Additionally, large biotite grains from MMEs definitely represent granitic xenocrysts as they show the same chemical composition (Fig. 8) and textural characteristics (Figs. 4, 5).

To constrain the origin of the mafic magma is difficult. The absence of olivine, pyroxene and amphibole even in the larger enclaves suggests that the mafic magma was nearly phenocryst free when intruding into the granite. The few phenocrysts were completely transformed to biotite during mixing with the granite even though not a single pseudomorphic relic was observed. Biotite, quartz and amphibole observed in the reaction texture (Fig. 5d) could be the remnant of such a reaction, and the more mafic composition of this biotite is supportive of that (see Fig. 8). Alternatively, the mafic magma was not primitive, but hybridized as a result of contamination in the lower crust

(e.g. Koteas et al. 2010) or (at least partly) at the emplacement level (e.g. Altherr et al. 1999).

Based on the conclusion that the formation of granitic melts in the Schwarzwald was likely caused either by underplating of mantle-derived melts or by asthenospheric upwelling associated with delamination (Büttner and Kruhl 1997; Marschall et al. 2003), interaction between mafic and silicic magmas could already have occurred in the lower crust associated with the generation of mafic enclaves in granitic partial melts (e.g. Koteas et al. 2010). However, during adiabatic rise to the depth of intrusion, enclaves can easily be “digested” and obliterated and only some crystals remain (Barbarin and Didier 1992; Furman and Spera 1985). Consequently, the well-preserved MMEs of the Albtal granite probably represent mixing between a granitic and a more mafic magma at the emplacement level.

Details of the mixing process as revealed by plagioclase textures and composition

In general, normal zonation of plagioclase reflected by decreasing An contents from core to rim would be expected in the case of undisturbed fractional crystallization with decreasing temperature in a closed system. On the contrary, reverse zonation implies a disturbance of the normal crystallization process. Parameters controlling the An content of plagioclase are temperature, pressure, fluid pressure and melt composition (e.g. Cashman and Blundy 2013; Couch et al. 2001, 2003; Lange et al. 2009; Panjasawatwong et al. 1995; Ustunisik et al. 2014). The qualitative effect of these parameters is rather easy to assess (Fig. 11a), but quantification is difficult and often depends on the bulk composition of the considered system. Furthermore, a change in different parameters may result in the same effect. For instance, rising temperature, increasing H_2O content or a more mafic magma chemistry all result in an increase in the An content. In contrast, the Sr content of plagioclase mostly depends on the parental magma and the plagioclase composition, but only to a minor degree on the temperature (Blundy and Wood 1991). Hence, the calculated Sr content of the corresponding melt is indicative of compositional variations in the magma chamber.

Figure 11b summarizes the data of all analysed profiles and shows that an interpretation based solely on the crystals' Sr content might lead to wrong conclusions because no clear relationship between the An and Sr content is visible. Therefore, the calculated Sr content of the parental melt is plotted versus the An content of plagioclase (Fig. 11c). Analyses of granite plagioclase (using a melt temperature of 750 °C for the calculations) cluster around An_{30} and Sr_{melt} contents vary between 30–110 ppm, resulting in a vertical trend in the plot termed “granite effect”. Although the melt differentiates as reflected by the decreasing Sr

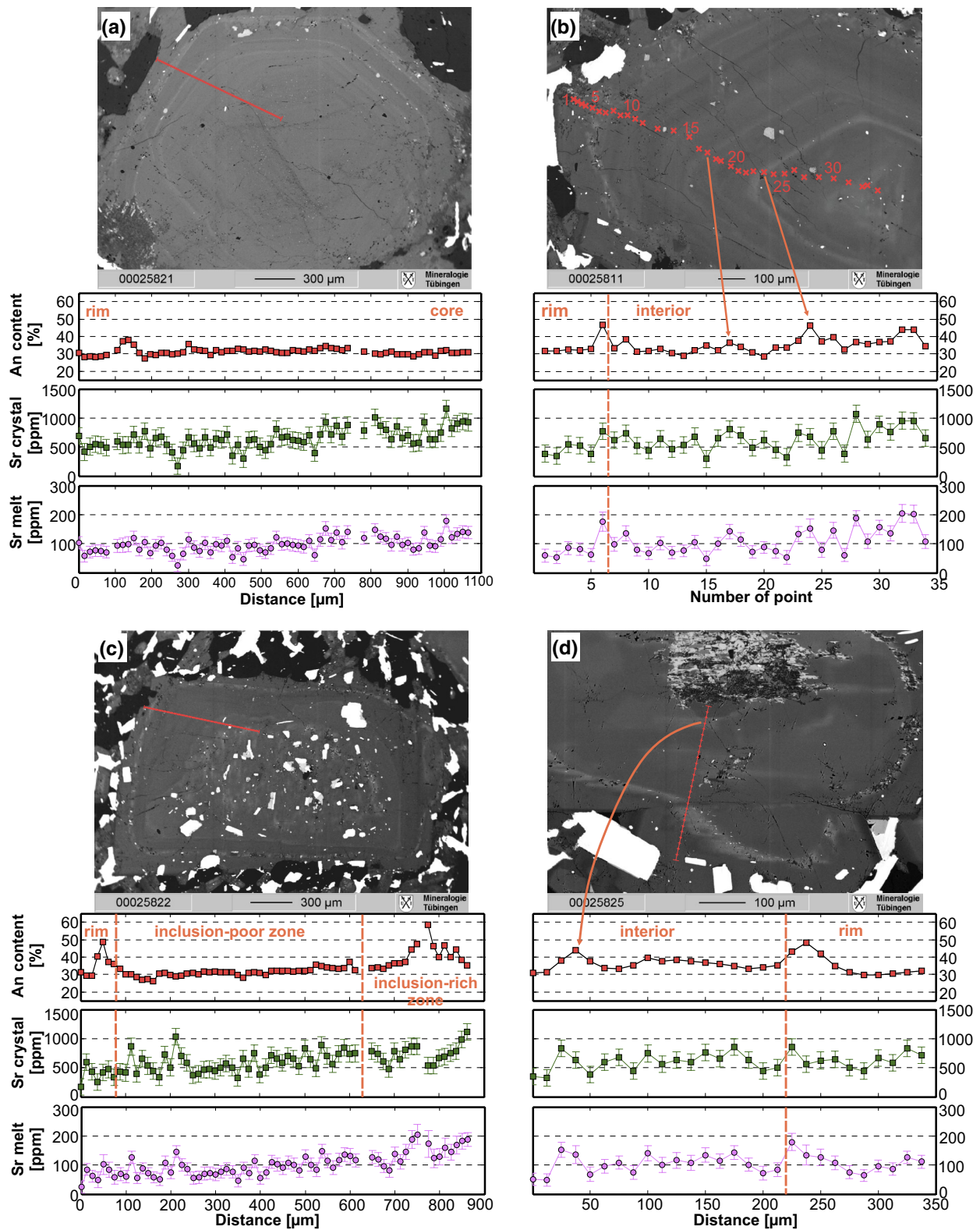


Fig. 10 Chemical profiles of different plagioclase types from the granite **a**, and the MMEs: **b** zoned type, **c** inclusion-rich type, **d** core type. The plots show the An and the Sr content of the crystal and the calculated Sr content of the parental melt using a temperature of

900 °C (see text for details). Note that a calculation at 750 °C would be within the analytical uncertainty of the microprobe analyses. *Distinct domains* in the single grains are indicated in the plots

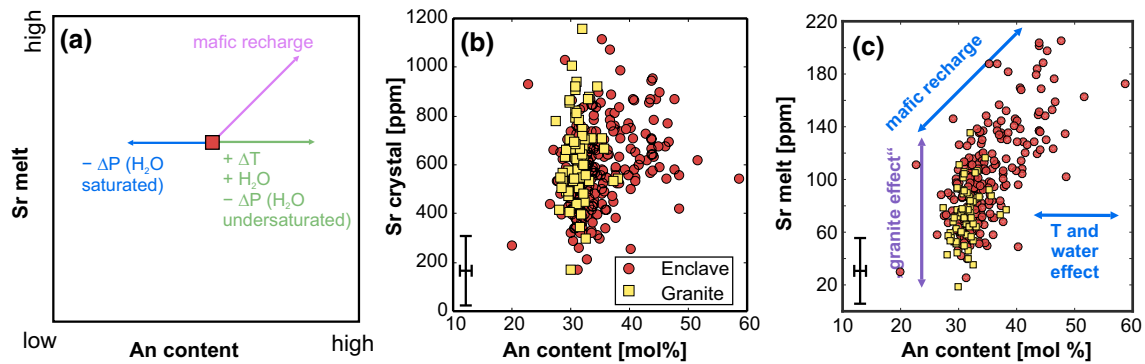


Fig. 11 **a** Schematic sketch of the qualitative effects of changes in pressure (ΔP), temperature (ΔT) and melt chemistry on the plagioclase composition (An content, calculated Sr content of the melt). **b** Summary of all plagioclase analyses performed in the different MME plagioclase types ($n = 254$) and the granite plagioclase ($n = 72$), comparing the An content with the measured Sr content of plagioclase

contents, the An content stays rather constant, probably due to depletion of the melt in Ca and Sr, but enrichment in water with ongoing plagioclase crystallization. This favours a higher An content of plagioclase, outbalancing the decreasing effect of Ca depletion in the melt and decreasing temperatures.

An₃₀–An₃₅ is the dominating An content in most of the MMEs' plagioclase types, being very similar to the plagioclase composition in the granite (Fig. 11c). For most of them, 30–120 ppm Sr was calculated using a temperature of 900 °C for the related melts, very similar to the calculated Sr content of the granitic melt. We interpret this as a strong hint that a great portion of large plagioclase crystals crystallized from the granitic melt. On the other hand, An-rich zones in the interior of the plagioclase grains and the thin An₅₀ seams of the rims often coincide with a significantly higher Sr content of the melt (up to 210 ppm), which is indicative of replenishment with a mafic Sr-enriched magma (i.e. “mafic recharge”). Plagioclase zones only enriched in the An component probably formed due to a rise in temperature or water content (e.g. Pietranik and Koepke 2014).

The intensity of the reaction between “granitic” plagioclase and a more mafic magma batch increases from the zoned to the inclusion-rich type, because in the zoned plagioclase only partial resorption prior to An-rich overgrowths occurred, whereas in the inclusion-rich plagioclase the reaction was more vigorous. The patterns of inclusion-rich plagioclase are similar to that produced in the experiments of Nakamura and Shimakita (1998), who dissolved a sodic plagioclase in a more mafic melt. As a result, a reaction zone formed, which consisted of melt channels or pockets of angular shape filled with reacted, more calcic plagioclase. The strong reaction of inclusion-rich

plagioclase grains in the Albtal pluton was also caused by a more mafic magma as reflected by high Sr_{melt} values of the An-rich patches.

Core-type plagioclase grains contain rounded cores of very high An contents (An₆₅–An₇₀) that are overgrown by low-An regions of “granitic” composition and a high-An seam at the rim. At first sight, the cores could be expected to originate from the mafic magma. However, Humphreys et al. (2006) described a patchy-zoned plagioclase, caused by resorption of An-rich plagioclase during decompressional rise and subsequent growth of low-An plagioclase at lower pressure under water-saturated conditions, whereas the core-type plagioclase of the Albtal MMEs lacks patchy zoning and has a rounded core. More probably, the core-type plagioclase grains are of granitic origin and the cores are restitic plagioclase from the source region (Johannes and Holtz 1996).

A conceptual model for magma mixing in the Albtal pluton

If a more mafic magma of higher density and lower viscosity is injected in a less dense, more viscous granitic magma, the former will underplate the latter without significant interaction and mixing unless intrusion is very turbulent (Sparks and Marshall 1986). As a consequence of the heating from below, resorption or reaction of phenocrysts of the granitic reservoir magma near the interface is predicted (Eichelberger 1980) and actually reflected by various resorption patterns in quartz grains of MMEs (Fig. 7b) and partly also of the fine-grained granite from the Albtal pluton. However, mixing between the granitic and the more mafic magma is also recorded by the high-An and high Sr_{melt} zones, either as concentric growth zones in

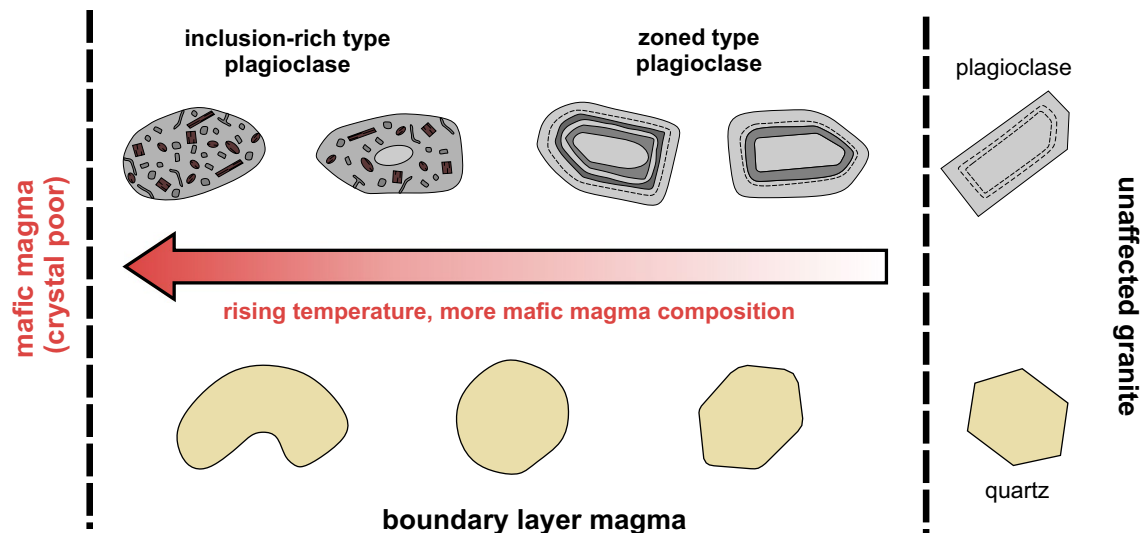


Fig. 12 Formation of the texturally different plagioclase and quartz types in a thermal and compositional gradient of the boundary layer magma by variable overprint of former granitic minerals. A lighter grey in the plagioclase corresponds to a lower An content

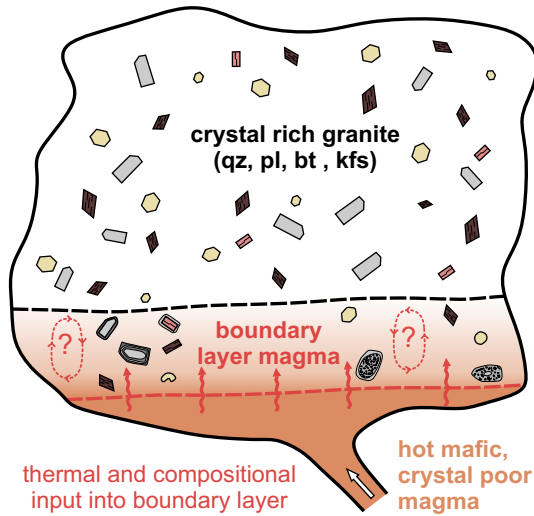
the interior of zoned-type plagioclase or as small patches in inclusion-rich grains. The different degree of overprint of inclusion-rich and zoned plagioclase and also of “granitic” quartz xenocrysts is interpreted to depend on the distance to the mafic injection, i.e. the resulting compositional and temperature gradients (Fig. 12). A compositional gradient can also explain the return to granitic “background” compositions of An_{30} in the zoned and inclusion-rich plagioclase, if these crystals were convectively transported back to regions with more “granitic” composition. All processes mentioned above are referred to as the “phase I” of the interaction process (Fig. 13) and result in the formation of an area of overprinted granite termed boundary layer, as also suggested for other plutons (e.g. Wiebe et al. 1997). Temperatures inside the boundary layer did not exceed the stability limit of biotite, because all large, inclusion-rich biotites (which are interpreted as xenocrysts derived from the granite) do not show any signs of reaction or disequilibrium.

Formation of MMEs occurred during the “enclave phase” (Fig. 13). Instability of the boundary layer was likely caused by input of a new mafic magma batch into the boundary layer magma (see, e.g. Weidendorfer et al. 2014 for similar complex scenarios with several mafic pulses and variable proportions of felsic and mafic magmas). Input of new mafic magma is reflected by thin seams of An_{50} with higher calculated Sr_{melt} values in almost all large MME plagioclase grains. Compared to the “normal” granite magma, the lowered viscosity of the hybridized and heated boundary layer magma had enhanced capabilities to mix with the intruding mafic magma (Sparks and Marshall 1986). The following two

scenarios may explain the formation of the MMEs: Due to the higher temperature of the injected mafic magma, fluid exsolution and vesiculation of the boundary layer magma could cause foaming (e.g. Coombs et al. 2003; Eichelberger 1980). The resulting decrease in density caused higher buoyancy, disruption of the boundary layer magma and the rise of magma blobs into the granitic magma, where further dispersal in enclaves took place. However, we did not observe vesicles in our samples. The break-up of the boundary layer magma was more likely caused by convection in the granite magma or by very forceful injection of the new mafic magma (cf. Coombs et al. 2003).

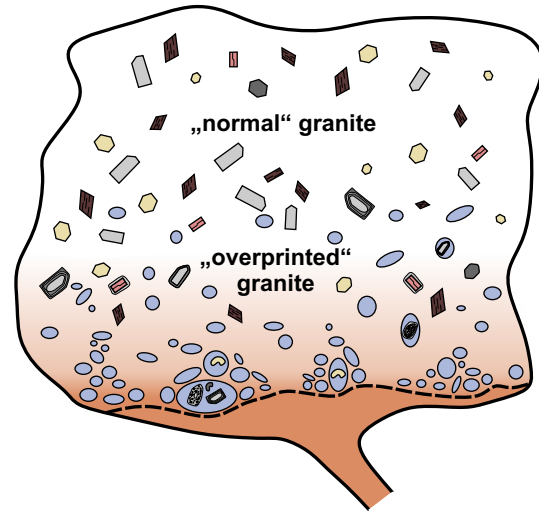
Due to the buoyant rise of the enclaves, they were transported to the “normal” granite. This sudden change in the crystallization conditions is evidenced by the rapid decrease in the An content of plagioclase rims back to the granite background value of An_{30} . Caused by the lower temperature of the granitic magma, thermal quenching of the MMEs is indicated by the presence of needle apatite (Wyllie et al. 1962) in the rims of large and matrix plagioclase and coarse-grained quartz. Thermal quenching also resulted in formation of the enclaves’ matrix, consisting of plagioclase, biotite and quartz. This has important implications for a further interaction between MMEs and the granite magma. The stability and rigidity of enclaves depends on the amount of melt left inside the enclave (e.g. Clynne 1999) and the development of a crystal framework, particularly of plagioclase (Martin et al. 2006). This inhibits disaggregation of the enclaves in the granite and explains their well-preserved shape. A largely crystallized and rigid enclave is also less capable of exchanging

**phase I:
heat up phase**



- development of a gradient
- remelting and reaction of crystals
- development of different plagioclase types
- An-rich seams in plagioclase
- maybe onset of convection

**phase II:
enclave phase**



- disruption of the boundary layer
- enclave formation
- dispersal of enclaves (buoyancy, convection)
- overprinted granite (rounded qz, rapakivi kfs, zoned/resorbed pl)

Mineral Legend:

- plagioclase
- alkali feldspar
- quartz
- biotite

- rapakivi feldspar
- inclusion-rich type plagioclase
- zoned type plagioclase

Fig. 13 Sketch of the MME-forming processes in the Albtal granite magma chamber. *Phase I* an intruding mafic magma leads to formation of a boundary layer magma that suffered from thermal overprint and chemical input from the mafic magma. Already present granitic minerals react and complex mineral textures originate (rounded quartz, zoned-type plagioclase, inclusion-rich type plagioclase).

Phase II This boundary layer magma disrupts due to a repeated input of mafic magma, leading to the formation and dispersal of blobs of MME magma. The granite with the fine-grained matrix, rounded quartz and rapakivi-type feldspar grains represents the upper part of the boundary layer magma

crystals with the surrounding granite. This is corroborated by the fact that almost all large plagioclase grains show the same pattern of their rims obtained prior to or during the break-up of the boundary layer, which one would not expect if plagioclase had been incorporated into the MMEs at different stages.

Impact of magma mixing on the Albtal granite

The upper part of the boundary layer magma suffered least from the input of the mafic magma. The observed fine-grained granite is interpreted to be derived from this part. Thermal and subordinate compositional overprint resulted in rounded quartz grains, rapakivi feldspar, strongly zoned

plagioclase and in its fine matrix. These features are not observed in the normal, coarse-grained granite. This region within the entire pluton is also the compositionally most primitive part of the Albtal granite (Emmermann 1968), indicating the influence of magma mixing on the observed tendencies towards an I-type signature.

Summary and conclusions

The results of detailed textural and mineral-chemical analyses of granite and mafic magmatic enclaves (MME) from the Variscan Albtal granite in SW Germany allow drawing the following conclusions:

1. MMEs in the Albtal granite are the product of interaction between a more mafic and a granitic magma.
2. Intrusion of the mafic magma into the granitic magma chamber resulted in the formation of a boundary layer that experienced mostly thermal and chemical input from the mafic magma. As a consequence, “granitic minerals” such as plagioclase and quartz were partly corroded and eventually recrystallized, whereas biotite did not react. The several large plagioclase types (inclusion-rich, core and zoned types) reflect different degrees of overprint along thermal and compositional gradients.
3. Break-up of the boundary layer occurred during the forceful intrusion of a second mafic magma batch recorded by a thin An₅₀ seam with high calculated Sr_{melt} values in the rims of all large plagioclase types. The dispersal of the hot hybrid magma blobs in the cooler granite led to thermal quenching and formation of the enclaves expressed by numerous inclusions of needle apatite in the rims of large plagioclase and quartz grains and in the fine-grained enclave matrix.
4. Interaction of two contrasting magmas in the Albtal pluton caused also textural and chemical variations in the granite itself as recorded by rapakivi-type feldspar phenocrysts in fine-grained granite and tendencies towards I-type characteristics.

Acknowledgments Simone Kaulfuß is thanked for preparing the thin sections. Wolfgang Siebel, two anonymous reviewers and Editor Wolf-Christian Dullo gave thoughtful comments that improved the paper.

References

- Altherr R, Henjes-Kunst F, Langer C, Otto J (1999) Interaction between crustal-derived felsic and mantle-derived mafic magmas in the Oberkirch pluton (European Variscides, Schwarzwald, Germany). *Contrib Mineral Petrol* 137:304–322. doi:10.1007/s004100050552
- Barbarin B (2005) Mafic magmatic enclaves and mafic rocks associated with some granitoids of the central Sierra Nevada batholith, California: nature, origin, and relations with the hosts. *Lithos* 80:155–177 <http://dx.doi.org/10.1016/j.lithos.2004.05.010>
- Barbarin B, Didier J (1992) Genesis and evolution of mafic microgranular enclaves through various types of interaction between coexisting felsic and mafic magmas. *Earth Environ Sci Trans R Soc Edinb* 83:145–153. doi:10.1017/S0263593300007835
- Bateman R, Martín MP, Castro A (1992) Mixing of cordierite granitoid and pyroxene gabbro, and fractionation, in the Santa Olalla tonalite (Andalucía). *Lithos* 28:111–131. doi:10.1016/0024-4937(92)90027-V
- Blundy JD, Shimizu N (1991) Trace element evidence for plagioclase recycling in calc-alkaline magmas. *Earth Planet Sci Lett* 102:178–197. doi:10.1016/0012-821X(91)90007-5
- Blundy JD, Wood BJ (1991) Crystal-chemical controls on the partitioning of Sr and Ba between plagioclase feldspar, silicate melts, and hydrothermal solutions. *Geochim Cosmochim Acta* 55:193–209. doi:10.1016/0016-7037(91)90411-W
- Brophy JG, Dorais MJ, Donnelly-Nolan J, Singer BS (1996) Plagioclase zonation styles in hornblende gabbro inclusions from Little Glass Mountain. Medicine Lake volcano, California: implications for fractionation mechanisms and the formation of composition gaps. *Contrib Mineral Petrol* 126:121–136. doi:10.1007/s004100050239
- Büsch W, Otto J (1980) Endogenetic inclusions in granites of the Black Forest, Germany *Neues Jahrbuch für Mineralogie, Monatshefte* 269–282
- Büttner S, Kruhl JH (1997) The evolution of a late-Variscan high-T/low-P region: the southeastern margin of the Bohemian massif. *Geol Rundsch* 86:21–38. doi:10.1007/s005310050119
- Cashman K, Blundy J (2013) Petrological cannibalism: the chemical and textural consequences of incremental magma body growth. *Contrib Mineral Petrol* 166:703–729. doi:10.1007/s00410-013-0895-0
- Chappell BW (1996) Magma mixing and the production of compositional variation within granite suites: evidence from the granites of Southeastern Australia. *J Petrol* 37:449–470. doi:10.1093/ptrology/37.3.449
- Clemens JD, Stevens G (2012) What controls chemical variation in granitic magmas—a signal from the source? *Lithos* 134–135:317–329. doi:10.1016/j.lithos.2012.01.001
- Clemens JD, Helps PA, Stevens G (2009) Chemical structure in granitic magmas—a signal from the source? *Earth Environ Sci Trans R Soc Edinb* 100:159–172. doi:10.1017/S1755691009016053
- Clynne MA (1999) A complex magma mixing origin for rocks erupted in 1915 Lassen Peak, California. *J Petrol* 40:105–132. doi:10.1093/ptrology/40.1.105
- Coombs ML, Eichelberger JC, Rutherford MJ (2003) Experimental and textural constraints on mafic enclave formation in volcanic rocks. *J Volcanol Geotherm Res* 119:125–144. doi:10.1016/S0377-0273(02)00309-8
- Couch S, Sparks RSJ, Carroll MR (2001) Mineral disequilibrium in lavas explained by convective self-mixing in open magma chambers. *Nature* 411:1037–1039
- Couch S, Harford CL, Sparks RSJ, Carroll MR (2003) Experimental constraints on the conditions of formation of highly calcic plagioclase microlites at the Soufrière Hills volcano, Montserrat. *J Petrol* 44:1455–1475. doi:10.1093/ptrology/44.8.1455
- Davidson JP, Hora JM, Garrison JM, Dungan MA (2005) Crustal forensics in arc magmas. *J Volcanol Geotherm Res* 140:157–170. doi:10.1016/j.jvolgeoes.2004.07.019
- Didier J, Barbarin B (1991) The different types of enclaves in granites—nomenclature. In: Didier J, Barbarin B (eds) *Enclaves and granite petrology. Developments in petrology, vol 13*. Elsevier, Amsterdam, pp 19–23
- Eichelberger JC (1978) Andesitic volcanism and crustal evolution. *Nature* 275:21–27
- Eichelberger JC (1980) Vesiculation of mafic magma during replenishment of silicic magma reservoirs. *Nature* 288:446–450
- Eisbacher GH, Lüschen E, Wickert F (1989) Crustal-scale thrusting and extension in the Hercynian Schwarzwald and Vosges, central Europe. *Tectonics* 8:1–21. doi:10.1029/TC008i001p00001
- Emmermann R (1968) Differentiation und Metasomatose des Albtalgranits (Südschwarzwald). *N Jahrb Mineral Abh* 109:96–130
- Emmermann R, Daieva L, Schneider J (1975) Petrologic significance of rare earths distribution in granites. *Contrib Mineral Petrol* 52:267–283. doi:10.1007/BF00401457
- Eroglu S, Schoenberg R, Wille M, Beukes N, Taubald H (2015) Geochemical stratigraphy, sedimentology, and Mo isotope systematics of the ca. 2.58–2.50 Ga-old transvaal supergroup carbonate platform, South Africa. *Precambrian Res* 266:27–46. doi:10.1016/j.precamres.2015.04.014
- Farner MJ, Lee C-TA, Putirka KD (2014) Mafic–felsic magma mixing limited by reactive processes: a case study of biotite-rich rinds on mafic enclaves. *Earth Planet Sci Lett* 393:49–59. doi:10.1016/j.epsl.2014.02.040
- Flood RH, Shaw SE (2014) Microgranitoid enclaves in the felsic Looanga monzogranite, New England Batholith,

- Australia: pressure quench cumulates. *Lithos* 198–199:92–102. doi:[10.1016/j.lithos.2014.03.015](https://doi.org/10.1016/j.lithos.2014.03.015)
- Furman T, Spera FJ (1985) Co-mingling of acid and basic magma with implications for the origin of mafic I-type xenoliths: field and petrochemical relations of an unusual dike complex at eagle lake, Sequoia National Park, California, U.S.A. *J Volcanol Geotherm Res* 24:151–178. doi:[10.1016/0377-0273\(85\)90031-9](https://doi.org/10.1016/0377-0273(85)90031-9)
- Hann HP, Chen F, Zedler H, Frisch W, Loeschke J (2003) The Rand granite in the southern Schwarzwald and its geodynamic significance in the Variscan belt of SW Germany. *Int J Earth Sci* 92:821–842. doi:[10.1007/s00531-003-0361-8](https://doi.org/10.1007/s00531-003-0361-8)
- Hegner E, Chen F, Hann HP (2001) Chronology of basin closure and thrusting in the internal zone of the Variscan belt in the Schwarzwald, Germany: evidence from zircon ages, trace element geochemistry, and Nd isotopic data. *Tectonophysics* 332:169–184. doi:[10.1016/S0040-1951\(00\)00254-7](https://doi.org/10.1016/S0040-1951(00)00254-7)
- Hibbard MJ (1991) Textural anatomy of twelve magma-mixed granitoid systems. In: Didier J, Barbarin B (eds) *Enclaves and granite petrology*. Developments in petrology, vol 13. Elsevier, London, pp 431–444
- Hibbard MJ (1995) *Petrography to petrogenesis*, 1st edn. Prentice Hall, Upper Saddle River
- Hoefs J, Emmermann R (1983) The oxygen isotope composition of Hercynian granites and pre-Hercynian gneisses from the Schwarzwald, SW Germany. *Contrib Mineral Petrol* 83:320–329. doi:[10.1007/BF00371200](https://doi.org/10.1007/BF00371200)
- Hogan JP (1993) Monomineralic glomerocrysts: textural evidence for mineral resorption during crystallization of igneous rocks. *J Geol* 101:531–540. doi:[10.2307/30068805](https://doi.org/10.2307/30068805)
- Humphreys MCS, Blundy JD, Sparks RSJ (2006) Magma evolution and open-system processes at Shiveluch volcano: insights from phenocryst zoning. *J Petrol* 47:2303–2334. doi:[10.1093/ptrology/egl045](https://doi.org/10.1093/ptrology/egl045)
- Johannes W, Holtz F (1996) *Petrogenesis and experimental petrology of granitic rocks*. Minerals and rocks, vol 22. Springer, Heidelberg
- Kalt A, Grauert B, Baumann A (1994) Rb-Sr and U-Pb isotope studies on migmatites from the Schwarzwald (Germany): constraints on isotopic resetting during Variscan high-temperature metamorphism. *J Metamorph Geol* 12:667–680. doi:[10.1111/j.1525-1314.1994.tb00050.x](https://doi.org/10.1111/j.1525-1314.1994.tb00050.x)
- Koteas GC, Williams ML, Seaman SJ, Dumond G (2010) Granite genesis and mafic-felsic magma interaction in the lower crust. *Geology* 38:1067–1070. doi:[10.1130/g31017.1](https://doi.org/10.1130/g31017.1)
- Lange RA, Frey HM, Hector J (2009) A thermodynamic model for the plagioclase-liquid hygrometer/thermometer. *Am Mineral* 94:494–506. doi:[10.2138/am.2009.3011](https://doi.org/10.2138/am.2009.3011)
- LeMaitre RW (2002) *Igneous rocks: a classification and glossary of terms; recommendations of the International Union of Geological Sciences, Subcommittee on the Systematics of Igneous Rocks*, 2nd edn. Cambridge University Press, Cambridge
- Liew TC, Hofmann AW (1988) Precambrian crustal components, plutonic associations, plate environment of the Hercynian Fold Belt of central Europe: indications from a Nd and Sr isotopic study. *Contrib Mineral Petrol* 98:129–138. doi:[10.1007/BF00402106](https://doi.org/10.1007/BF00402106)
- Marschall HR, Kalt A, Hanel M (2003) P-t evolution of a variscan lower-crustal segment: a study of granulites from the Schwarzwald, Germany. *J Petrol* 44:227–253. doi:[10.1093/ptrology/44.2.227](https://doi.org/10.1093/ptrology/44.2.227)
- Martin VM, Pyle DM, Holness MB (2006) The role of crystal frameworks in the preservation of enclaves during magma mixing. *Earth Planet Sci Lett* 248:787–799. doi:[10.1016/j.epsl.2006.06.030](https://doi.org/10.1016/j.epsl.2006.06.030)
- Nakamura M, Shimakita S (1998) Dissolution origin and syn-entrapment compositional change of melt inclusion in plagioclase. *Earth Planet Sci Lett* 161:119–133. doi:[10.1016/S0012-821X\(98\)00144-7](https://doi.org/10.1016/S0012-821X(98)00144-7)
- Neves SP, Vauchez A (1995) Successive mixing and mingling of magmas in a plutonic complex of Northeast Brazil. *Lithos* 34:275–299. doi:[10.1016/0024-4937\(94\)00012-Q](https://doi.org/10.1016/0024-4937(94)00012-Q)
- Panjasawatwong Y, Danyushevsky L, Crawford A, Harris K (1995) An experimental study of the effects of melt composition on plagioclase-melt equilibria at 5 and 10 kbar: implications for the origin of magmatic high-An plagioclase. *Contrib Mineral Petrol* 118:420–432. doi:[10.1007/s004100050024](https://doi.org/10.1007/s004100050024)
- Perugini D, Poli G (2012) The mixing of magmas in plutonic and volcanic environments: analogies and differences. *Lithos* 153:261–277. doi:[10.1016/j.lithos.2012.02.002](https://doi.org/10.1016/j.lithos.2012.02.002)
- Pietranik A, Koepke J (2009) Interactions between dioritic and granodioritic magmas in mingling zones: plagioclase record of mixing, mingling and subsolidus interactions in the Gęsiniec intrusion NE Bohemian Massif, SW Poland. *Contrib Mineral Petrol* 158:17–36. doi:[10.1007/s00410-008-0368-z](https://doi.org/10.1007/s00410-008-0368-z)
- Pietranik A, Koepke J (2014) Plagioclase transfer from a host granodiorite to mafic microgranular enclaves: diverse records of magma mixing. *Mineral Petrol* 1–14 doi:[10.1007/s00710-014-0326-6](https://doi.org/10.1007/s00710-014-0326-6)
- Pietranik A, Waight TE (2008) Processes and sources during late Variscan Dioritic-Tonalitic magmatism: insights from plagioclase chemistry (Gęsiniec intrusion, NE Bohemian Massif, Poland). *J Petrol* 49:1619–1645. doi:[10.1093/ptrology/egn040](https://doi.org/10.1093/ptrology/egn040)
- Pietranik A, Koepke J, Puziewicz J (2006) Crystallization and resorption in plutonic plagioclase: implications on the evolution of granodiorite magma (Gęsiniec granodiorite, strzelin crystalline Massif, SW Poland) *Lithos* 86:260–280 <http://dx.doi.org/10.1016/j.lithos.2005.05.008>
- Pitcher WS (1997) *The nature and origin of granite*, 2nd edn. Chapman & Hall, London; Weinheim [u.a.]
- Reubi O, Blundy J (2009) A dearth of intermediate melts at subduction zone volcanoes and the petrogenesis of arc andesites. *Nature* 461:1269–1273
- Schaltegger U (2000) U-Pb geochronology of the Southern Black Forest Batholith (Central Variscan Belt): timing of exhumation and granite emplacement. *Int J Earth Sci* 88:814–828. doi:[10.1007/s005310050308](https://doi.org/10.1007/s005310050308)
- Schuler C (1983) *Die interne SR-Isotopensystematik des herzynischen Albtalgranits (Schwarzwald)*. Zürich, Techn. Hochsch., Diss., 1983, Zürich
- Singer BS, Dungan MA, Layne GD (1995) Textures and Sr, Ba, Mg, Fe, K and Ti compositional profiles in volcanic plagioclase clues to the dynamics of calc-alkaline magma chambers. *Am Mineral* 80:776–798
- Sisson TW, Grove TL, Coleman DS (1996) Hornblende gabbro sill complex at Onion valley, California, and a mixing origin for the Sierra Nevada batholith. *Contrib Mineral Petrol* 126:81–108. doi:[10.1007/s004100050237](https://doi.org/10.1007/s004100050237)
- Sparks RSJ, Marshall LA (1986) Thermal and mechanical constraints on mixing between mafic and silicic magmas. *J Volcanol Geotherm Res* 29:99–124. doi:[10.1016/0377-0273\(86\)90041-7](https://doi.org/10.1016/0377-0273(86)90041-7)
- Stenger R (1979) *Petrographie und Geochemie der endogenen Einschlüsse im Albtalgranit (Südschwarzwald)*. Jahresheft des geologischen Landesamtes Baden-Württemberg 21:89–106
- Ubide T, Galé C, Larrea P, Arranz E, Lago M, Tierz P (2014) The relevance of crystal transfer to magma mixing: a case study in composite dykes from the central pyrenees. *J Petrol* 55:1535–1559. doi:[10.1093/ptrology/egu033](https://doi.org/10.1093/ptrology/egu033)
- Ustunisik G, Kilinc A, Nielsen RL (2014) New insights into the processes controlling compositional zoning in plagioclase. *Lithos* 200–201:80–93. doi:[10.1016/j.lithos.2014.03.021](https://doi.org/10.1016/j.lithos.2014.03.021)
- Waight TE, Maas R, Nicholls IA (2001) Geochemical investigations of microgranitoid enclaves in the S-type Cowra Granodiorite, Lachlan Fold Belt, SE Australia. *Lithos* 56:165–186. doi:[10.1016/S0024-4937\(00\)00053-0](https://doi.org/10.1016/S0024-4937(00)00053-0)

- Weidendorfer D, Mattsson HB, Ulmer P (2014) Dynamics of Magma Mixing in Partially crystallized magma chambers: textural and petrological constraints from the basal complex of the austurhorn intrusion (SE Iceland). *J Petrol* 55:1865–1903. doi:[10.1093/petrology/egu044](https://doi.org/10.1093/petrology/egu044)
- Wiebe RA, Smith D, Sturm M, King EM, Seckler MS (1997) Enclaves in the Cadillac Mountain granite (coastal maine): samples of hybrid magma from the base of the chamber. *J Petrol* 38:393–423. doi:[10.1093/petroj/38.3.393](https://doi.org/10.1093/petroj/38.3.393)
- Wimmenauer W (1963) Einschlüsse im Albtalgranite (Südschwarzwald) und ihre Bedeutung für dessen Vorgeschichte. *Neues Jahrbuch für Mineralogie, Monatshefte* 1:6–17
- Wyllie PJ, Cox KG, Biggar GM (1962) The habit of apatite in synthetic systems and igneous rocks. *J Petrol* 3:238–243. doi:[10.1093/petrology/3.2.238](https://doi.org/10.1093/petrology/3.2.238)